

# Chemical Composition, Petrology and P-T Conditions of Ti-Mg-Biotites within Syenitic Rocks from the Lar Igneous Suite, East of Iran

Sasan Ghafaribijar, Javad Hakimi, Mohsen Arvin, Peyman Tahernezhad

**Abstract**—The Lar Igneous Suite (LIS), east of Iran, is part of post collisional alkaline magmatism related to Late Cretaceous- mid Eocene Sistan suture zone. The suite consists of a wide variety of igneous rocks, from volcanic to intrusive and hypabissal rocks such as tuffs, trachyte, monzonite, syenites and lamprophyres. Syenitic rocks which mainly occur in a giant ring dike and stocks, are shoshonitic to potassic-ultrapotassic ( $K_2O/Na_2O > 2$  wt.%;  $MgO > 3$  wt.%;  $K_2O > 3$  wt.%) in composition and are also associated with Cu-Mo mineralization. In this study, chemical composition of biotites within the Lar syenites (LS) is determined by electron microprobe analysis. The results show that LS biotites are Ti-Mg-biotites (phlogopite) which contain relatively high Ti and Mg, and low Fe concentrations. The  $Mg/(Fe^{2+} + Mg)$  ratio in these biotites range between 0.56 and 0.73 that represent their transitionally chemical evolution.  $TiO_2$  content in these biotites is high and in the range of 3.0-5.4 wt.%. These chemical characteristics indicate that the LS biotites are primary and have been crystallized directly from magma. The investigations also demonstrate that the LS biotites have crystallized from a magma of orogenic nature. Temperature and pressure are the most significant factors controlling Mg and Ti content in the LS biotites, respectively. The results show that the LS biotites crystallized at temperatures (T) between 800 to 842 °C and pressures (P) between 0.99 to 1.44 kbar. These conditions are indicative of a crystallization depth of 3.26-4.74 km

**Keywords**—Sistan suture zone, Lar Igneous Suite, Zahedan, syenite, biotite.

## I. INTRODUCTION

**B**IOTITE occurs in a great variety of rock types and its large range composition makes it a valuable source of information to estimate equilibrium conditions [1], [2] tectono-magmatic environment of its host-rock [3]-[5] and discriminate mineralized granitoid bodies from those which are barren [6], [7].

The composition of biotite phenocrysts appears to represent the chemical composition and P-T conditions of the host magma in which they have started to crystallize. The

S. Ghafaribijar is with the National Iranian Copper Industries Co. Sarcheshmeh Copper Complex. Islamic Republic of Iran (phone: +98-3430-2007; fax: +98-3430-2003; e-mail: sasan.ghb@gmail.com).

J. Hakimi is with the National Iranian Copper Industries Co. Sarcheshmeh Copper Complex. Islamic Republic of Iran (phone: +9834-3430-2007; fax: +9834-3430-2003).

M. Arvin is with the Geology Department, University of Shahid Bahonar, Kerman. Islamic Republic of Iran (phone: +9834-3132-2224; e-mail: Arvinm@yahoo.com).

P. Tahernezhad is with the National Iranian Copper Industries Co. Sarcheshmeh Copper Complex. Islamic Republic of Iran (phone: +9834-3430-2042; fax: +9834-3430-2003).

concentration of Ti and Al in biotite has long been considered as valuable functions to estimate the P-T conditions during magma crystallization [8], [9]. In this study, we focused on chemical composition of the LS phenocrystal biotites to clarify petrological characteristics and equilibrium conditions of biotites in the syenitic rocks which have intruded into the LIS, east of Iran.

## II. GEOLOGICAL SETTING

The Oligocene LIS is located in the Sistan suture zone (SSZ), east of Iran. The N-S trending SSZ represents a Tethys-related oceanic basin that has been closed during Late Cretaceous to Mid-Eocene times (Fig. 1). Its detailed tectonic history and subduction polarity of the Sistan Ocean is not well known [10]; however, the alkaline and calc-alkaline magmatism in the SSZ has been interpreted to be either of subduction [11], back-arc [12], or post-collisional origin [13], [14].

The LIS (22 km north of Zahedan), with a northwest trending, occupies an area adjacent to the junction of Iran, Afghanistan and Pakistan border. This suite represents perhaps the best combination of intrusive and extrusive exposure in the SSZ. They consist of an association of silica-undersaturated to nearly over-saturated rock types of various composition ranging from lamprophyres, Shonkinite, syenite, monzonite and nepheline syenite to tuffs and breccias (Fig. 1). Additionally, porphyry copper mineralization exists within the syenitic unit in the form of chalcopyrite, bornite, chalcocite and molybdenite.

The LS rocks crop out mainly as a ring dike and several stocks. The main syenitic ring dike is variable in size, width and dip through east to west of the suite. The rocks usually show inequigranular porphyritic texture except in the southwestern part of the ring dike with granular texture which is also associated with copper mineralization. The rocks range in composition from syenite to alkali-feldspare syenite. The Syenitic rocks contain megacrystal and phenocrystal K-feldspares which show magmatic foliation or flowing texture especially in western segment of the main ring dike.

In thin section, the LS rocks contain megacrystal and phenocrystal K-feldspare (55-75%), plagioclase (10-17%), biotite (12-20%), pyroxene (5-10%), amphibole (5-7%) and olivine (<5%) which are set in a medium to fine grained groundmass of all aforementioned minerals; apatite and titanite are the most common accessory minerals. Phenocrystal Biotites are pale brown to dark brown in color and strongly

pleochroic. These biotites become more elongated along western part of the main syenitic ring dike.

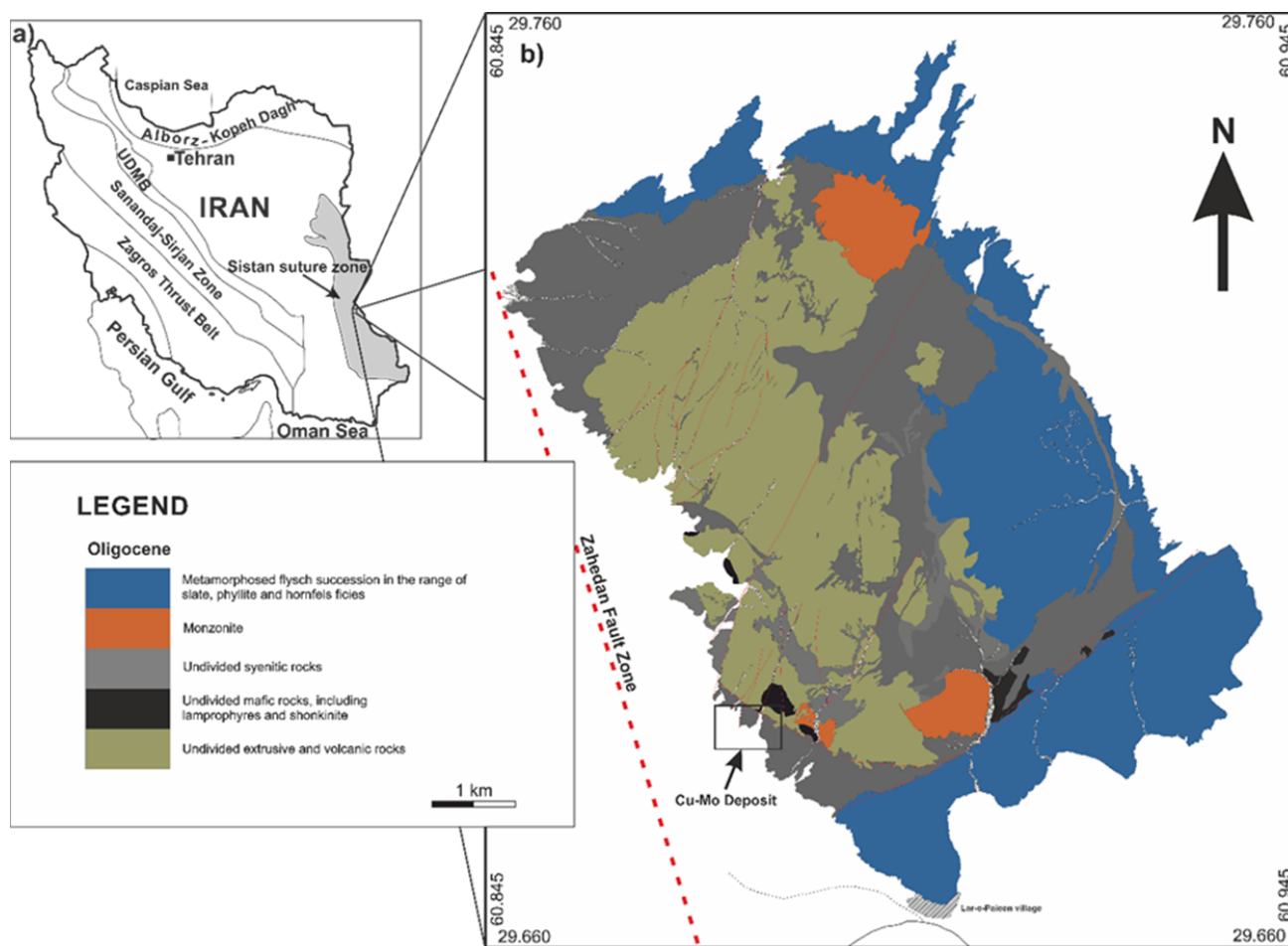


Fig. 1 (a) The main tectonostratigraphic map of Iran and the location of SSZ, (b) Geological map of LIS in the SSZ of eastern Iran showing important lithological and structural elements, and associated copper mineralization in the studying region

### III. ANALYTICAL METHODS

In this study, the chemical composition of biotite in 10 points from 5 syenitic rock samples were measured on polished thin sections using a camera SX-500 electron microprobe at the University of British Columbia. All compositions were determined under operating conditions of 15 kV and 20 n A, with peak counting times of 20 seconds. Off-peak background counts were collected for 10 seconds. A standard beam 2-5 μm in diameter was used for the analysis of biotite. The Biotite formula is based on the 22 oxygens and OH is calculated on OH=4-(Cl + F). Total iron in biotite is assumed as Fe<sup>2+</sup>. The syenitic rocks in the study area are shoshonitic to potassic-ultrapotassic (K<sub>2</sub>O/Na<sub>2</sub>O >2; MgO > 3 wt%; K<sub>2</sub>O > 3 wt %) in composition (Table I).

### IV. MINERAL CHEMISTRY

The EPMA results for LS biotites are listed in Table II. These results show that the LS biotites contain high concentrations of MgO (12.5–16.9 wt %) and relatively low

concentrations of Al<sub>2</sub>O<sub>3</sub> (13.7–14.4 wt %), with Mg/ (Fe<sup>2+</sup>+Mg) ratios that range between 0.56 and 0.73. TiO<sub>2</sub> concentration in these biotites is in the range of 3.0-5.4 wt%. The LS biotites also contain low concentrations of FeO (11.09– 17.45 wt %); the Fe/ (Fe<sup>2+</sup>+Mg) ratio in these biotites is 0.26-0.35. This large rang in Mg# and Fe/ (Fe<sup>2+</sup>+Mg) ratio demonstrates mineral evolution during magma fractionation. All of these characteristics imply that the LS biotites are primary and have been crystallized directly from magma [15].

TABLE I  
 CHEMICAL FEATURES OF THE LS ROCKS

Rock sample	LS	LS32	LS58	LS59	LS6
MgO wt%	4.18	1.84	3.77	2.09	4.44
K <sub>2</sub> O wt%	7.62	7.89	7.37	7.81	7.46
K <sub>2</sub> O/Na <sub>2</sub> O	2.01	1.8	1.68	1.81	1.99

TABLE II  
REPRESENTATIVE EPMA ANALYSES OF BIOTITE FROM THE LS ROCKS. THE BIOTITE FORMULA IS BASED ON THE 22 OXYGENS

Samples	LS58-C6-1	LS58-C8-1	LS 6-c1-1c	LS-c1-1c	LS-c3-1c	LS32-C3-1	LS32-C5-1c	LS59-c3-1c	LS59-c4-1c	LS59-c6-1c
SiO <sub>2</sub>	37.02	37.16	35.95	36.79	36.09	36.03	37.06	36.63	36.63	35.93
TiO <sub>2</sub>	5.46	5.29	3.07	3.48	3.27	3.07	4.73	4.92	3.76	3.85
Al <sub>2</sub> O <sub>3</sub>	14.20	14.16	13.78	14.40	14.28	13.87	14.88	14.00	14.42	14.17
Cr <sub>2</sub> O <sub>3</sub>	0.00	0.00	0.02	0.00	0.02	0.00	0.00	0.00	0.07	0.07
FeO	11.03	11.10	17.13	15.73	15.99	17.36	12.36	17.45	16.97	14.45
MnO	0.08	0.22	0.39	0.31	0.33	0.42	0.14	0.40	0.28	0.22
MgO	16.82	16.97	13.56	15.09	14.94	12.68	15.53	12.56	13.14	13.93
CaO	0.02	0.00	0.01	0.04	0.06	0.06	0.00	0.00	0.02	0.03
Na <sub>2</sub> O	0.63	0.44	0.31	0.68	0.56	0.41	0.58	0.36	0.36	0.30
K <sub>2</sub> O	9.60	9.72	9.85	9.58	9.50	9.06	9.19	9.85	9.53	9.48
F	0.68	0.35	0.14	0.38	0.04	0.33	0.43	0.10	0.25	0.26
Cl	0.08	0.05	0.04	0.02	0.02	0.06	0.04	0.03	0.00	0.03
H <sub>2</sub> O	3.68	3.85	3.78	3.80	3.90	3.65	3.78	3.89	3.81	3.72
Total	99.29	99.30	98.03	100.30	98.99	97.00	98.72	100.19	99.25	96.47
Si	5.451	5.464	5.520	5.471	5.443	5.578	5.490	5.496	5.525	5.524
Ti	0.000	0.000	0.000	0.000	0.000	0.000	0.000	0.000	0.000	0.000
Al (IV)	2.495	2.485	2.525	2.556	2.570	2.564	2.631	2.507	2.595	2.600
Total <sub>tet.</sub>	7.946	7.948	8.046	8.027	8.013	8.142	8.121	8.003	8.120	8.124
Al (VI)	0.000	0.000	0.000	0.000	0.000	0.000	0.000	0.000	0.000	0.000
Ti	0.810	0.820	0.842	0.817	0.808	0.783	0.792	0.837	0.822	0.817
Fe	1.375	1.382	2.228	1.981	2.043	2.276	1.551	2.218	2.167	1.881
Mn	0.010	0.027	0.051	0.039	0.043	0.056	0.018	0.051	0.037	0.029
Mg	3.738	3.766	3.144	3.388	3.401	2.963	3.474	2.845	2.992	3.234
Total <sub>oct.</sub>	5.933	5.995	6.265	6.225	6.295	6.079	5.835	5.951	6.018	5.961
Na	0.183	0.128	0.092	0.198	0.165	0.124	0.169	0.107	0.108	0.091
K	1.826	1.847	1.955	1.841	1.851	1.813	1.759	1.910	1.857	1.882
A site	2.010	1.975	2.047	2.039	2.016	1.937	1.927	2.017	1.965	1.973
F	0.322	0.164	0.070	0.180	0.017	0.163	0.202	0.048	0.122	0.130
Cl	0.021	0.013	0.011	0.005	0.005	0.015	0.011	0.009	0.000	0.008
OH	3.656	3.823	3.919	3.815	3.978	3.821	3.787	3.943	3.878	3.861
Fe/(Fe+Mg)	0.267	0.266	0.318	0.295	0.294	0.337	0.288	0.351	0.334	0.309
Mg/(Fe+Mg)	0.731	0.732	0.585	0.631	0.625	0.566	0.691	0.562	0.580	0.632

Open Science Index, Geological and Environmental Engineering Vol:13, No:7, 2019 publications.waset.org/10010600/pdf

The plot of Fe/(Fe<sup>2+</sup>+Mg) vs. total Al (apfu) [16] shows that the chemical composition of LS phenocrystal biotites are transitionally evolved to Fe-rich compositions (Fig. 2). According to this diagram, almost all LS biotites are classified as biotite of Mg-rich (Phlogopite). Reference [4] used mica composition to discriminate magma types in which they crystallized. In total Al (apfu) vs. Mg (apfu) classification diagram, the nature of granitoid magmas was grouped into four types such as peraluminous, calc-alkaline, sub-alkaline, and alkaline-Peralkaline (Fig. 3). Based on this diagram, the LS biotites are plotted in the field of Calc-alkaline magmas (Fig. 3). Reference [17] used a discrimination FeO<sub>t</sub>-MgO-Al<sub>2</sub>O<sub>3</sub> triangle diagram for biotites in igneous rocks crystallized from peraluminous, calc-alkaline and alkaline magmas (Fig. 4). In this diagram, the LS biotites also plotted in the field of Calc-alkaline magmas with orogenic affinities. The Al<sub>2</sub>O<sub>3</sub> content in the LS biotites prevent them to plot in the field of alkaline magmas; while the most syenitic rocks in the study area are alkaline and have high Al<sub>2</sub>O<sub>3</sub> and K<sub>2</sub>O/Na<sub>2</sub>O ratios (1-2). These rocks, according to [18], classify as Roman Province Type (RPT) or group 3 of potassic and ultrapotassic rocks.

The K<sub>2</sub>O/Na<sub>2</sub>O ratio in LS rocks decreases with

differentiation, so it is inconceivable to accept parental calc-alkaline magmas have undergone differentiation to produce potassic magmas. The RPT potassic- ultrapotassic rocks are also characterized by high Al<sub>2</sub>O<sub>3</sub> contents. In other word, the composition of biotite depends principally on the bulk composition [1], so the LS biotites have inherited their high Al contents from the host magma.

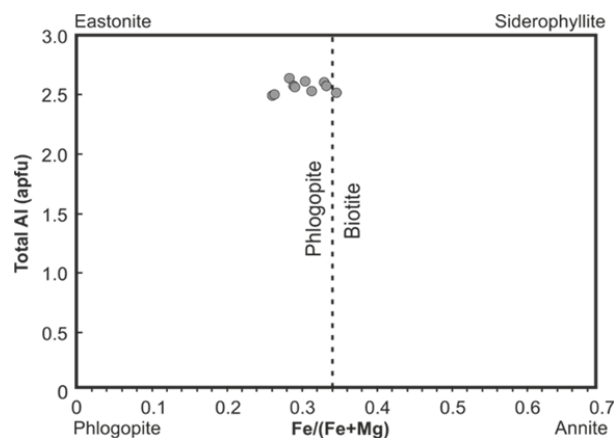


Fig. 2 Classification of biotite based on [16].

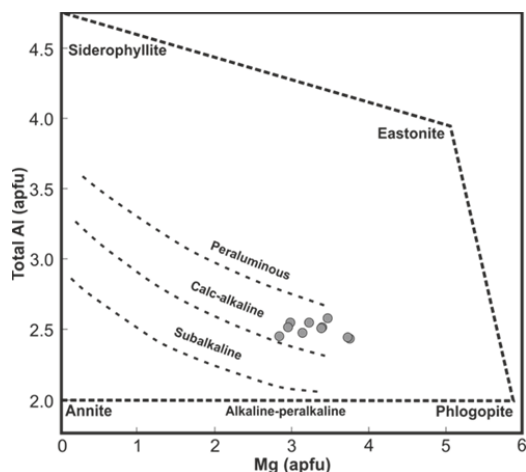


Fig. 3 Biotites from the study area plotted in diagram after [4] to discriminate the type of magma

#### V. TEMPERATURE AND PRESSURE

The concentration of Ti in biotite has considered to be sensitive to changing temperature so it has been recommended as a reliable geothermometer [5], [8], [19]-[22]. The factors that influence the incorporation of Ti in biotite are complex and involve temperature, pressure, crystal chemistry and coexisting mineral assemblages [8], [23], [24]. The temperature effect, however, appears to be the most influential factor. In phlogopite, the incorporation of Ti is relatively dramatic at high temperatures, particularly higher than 800 °C [8]. Reference [21] found that Ti content in phlogopite is relatively low (0.07 Ti apfu) at 600 °C, but increases significantly to 0.2 Ti (apfu) at 800 °C, and to 0.7 Ti (apfu) at 1000 °C. According to Table I, Si in LS biotites is replaced just by Al<sup>IV</sup> which indicates crystallization at high temperatures [16]. Reference [8] experimentally proposed that temperatures can be determined either by plotting Ti and Mg/(Mg + Fe) values in biotite (Fig. 5) or by calculating temperatures directly from the following expression:

$$T = \{[\ln(Ti) - a - c(X_{Mg})^3]/b\}^{0.333} \quad (1)$$

where T is the temperature, Ti is the apfu normalized to 22 oxygens,  $X_{Mg}$  is Mg/(Mg+Fe), and the b and c parameters are (-2.3594), (4.6482\*10<sup>-9</sup>) and (-1.7283), respectively. According to this equation, the crystallization temperature of LS biotites is in the range of 800-842 °C. In the plot of Mg/(Mg+Fe) vs. Ti (apfu) all LS biotites show crystallization temperatures higher than 800 °C. The highest temperature is related to sample LS58-C8-1 with highest Mg/(Mg+Fe) ratio, while there is no correlation between Ti and Mg/(Mg+Fe) in the study biotites.

Reference [25] experimentally documented a strong positive correlation between the total Al content of a biotite sample and the solidification pressure (P) of the granitic host rocks; their results lead to the following empirical equation:

$$P \text{ (kb)} = 3.03 \times Al_t - 6.53 (\pm 0.33) \quad (2)$$

where Al<sub>t</sub> is the total Al content of the biotite calculated based on 22 oxygens.

By using this geobarometer equation, we are able to estimate the pressure during crystallization of LS rocks. The results show that the pressure is 0.99-1.44 kbar, equating to depth of 3.26-4.74 km.

In the LS biotites, Mg/(Mg+Fe) ratio shows positive correlation with temperature, while their Ti content represents relatively negative correlation with pressure, which is consistent with results of [26] and [27]. In the other hand, the Mg/(Mg+Fe) ratio and Ti concentration in the LS biotites increase with increasing temperature and decreasing pressure, respectively.

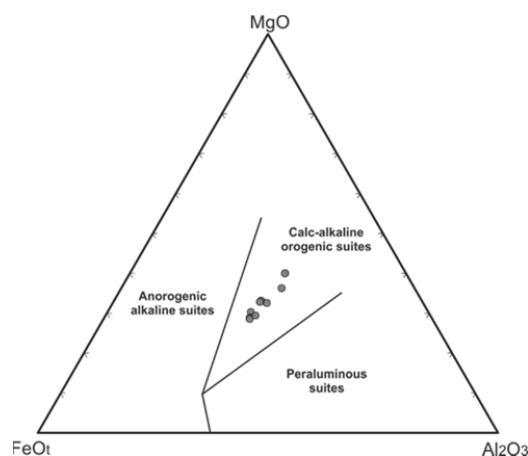


Fig. 4 Distribution of micas on ternary MgO-FeO-Al<sub>2</sub>O<sub>3</sub> tectonomagmatic discrimination diagram after [17]

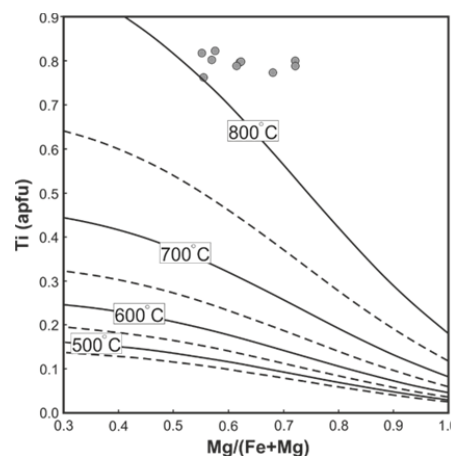


Fig. 5 Variations in the Ti vs. Mg/(Mg + Fe) ratio of biotites in the LS rocks; diagram after [8]

#### VI. CONCLUSION

The composition of LS phenocrystal biotites are enriched in Mg and Ti, and depleted in Fe. These features indicate that they are primary and magmatic phlogopites. We propose here that the LS biotites have crystallized from a magma within an orogenic tectonic setting. By using some discrimination diagrams, the nature and composition of the magmas in which the LS biotites have been crystallized, stand in the field of

orogenic calc-alkaline magmas, while the host syenitic rocks are alkaline and potassic-ultrapotassic in composition. The high Al content of their host magmas, due to their orogenic nature, is responsible for this inconsistency.

In LS biotites,  $\text{Si}^{4+}$  in the tetrahedral site is replaced by  $\text{Al}^{\text{IV}}$  not  $\text{Al}^{\text{VI}}$ , which indicates crystallization at high temperatures. In addition, the high Ti content in these biotites is another

indicator that denotes crystallization at high temperatures. There is a negative correlation between Ti content and pressure which implies that pressure is another dominant factor controlling Ti concentration in the LS biotites. The LS biotites crystallized at temperatures between 800 to 842 °C and pressures between 0.99 to 1.44 kbar, corresponding to depth of 3.26-4.74 km.

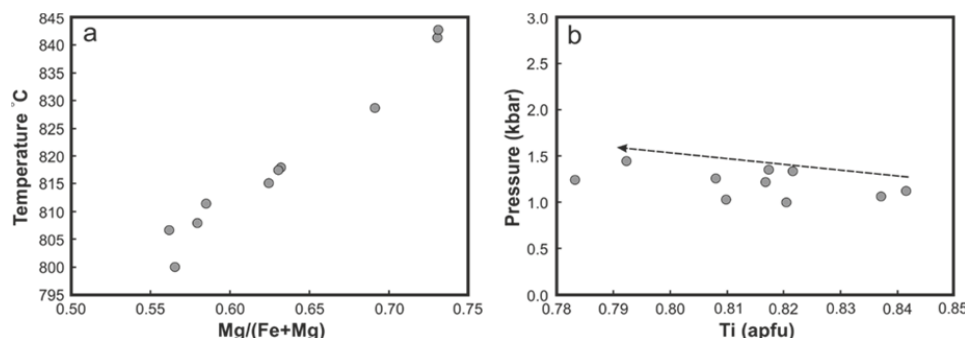


Fig. 6 (a) Variation in temperature (T) vs. Mg/ (Fe+Mg) ratio, (b) Variation in pressure (kbar) vs. Ti (apfu) for biotites in the LS rocks

#### REFERENCES

- [1] Labotka, T. C., (1983). Analysis of the compositional variations of biotite in pelitic hornfels from northeastern Minnesota. *American Mineralogist*, 68, 900-914.
- [2] Speer, J. A., (1984). Micas in igneous rocks. In: *Micas*. Bailey S.W., (Eds.). *Review of Mineralogy*, 13: 299-356.
- [3] Wones, D. R., Eugester, H. P., (1965). Stability of biotite: experiment, theory, and application. *American Mineralogist*, 50, 1228-1272.
- [4] Nachit, H., Razafimahefa, N., Stussi, J. M., Carron, J. P., (1985). Composition chimique des biotites et typologie magmatique des granitoids, *Comptes Rendus Hebdomadaires de l'Academie des Sciences* 301, 11, 813-818.
- [5] Patiño Douce, A. E., (1993). Titanium substitution in biotite: an empirical model with applications to thermometry,  $\text{O}_2$  and  $\text{H}_2\text{O}$  barometries, and consequences for biotite stability. *Chemical Geology*, 108, 133-162.
- [6] Boomeri, M., Mizuta, T., Ishiyama, D., Nakashima, K., (2006). Fluorine and chlorine in biotite from the Sarnowsar granitic rocks, Northeastern Iran. *Iranian Journal of Science & Technology, Transaction A*, 30, A1, 111-125.
- [7] Müller, D., Groves, D. I., (2016). *Potassic Igneous Rocks and Associated Gold-Copper Mineralization*. 4th edn. Springer- Mineral Resource Reviews, USA, 342p.
- [8] Henry, D. J., Guidotti, C. V., Thomsen, J. A., (2005). The Ti-saturation surface for low-to-medium pressure metapelitic biotites: implications for geothermometry and Ti-substitution mechanisms. *American Mineralogist*, 90, 316-328.
- [9] Dong, Q., Du, Y., Pang, Z., Miao, W., Tu, W., (2014). Composition of biotite within the Wushan granodiorite, Jiangxi Province, China: Petrogenetic and metallogenetic implications. *Earth Sciences Research Journal*, 18, 1, 39-44.
- [10] Richards, J. P., (2015). Tectonic, magmatic, and metallogenetic evolution of the Tethyan orogen: From subduction to collision. *Ore Geology Reviews*, 323-345.
- [11] Richards, J. P., Spell, T., Rameh, E., Raziq, A., Fletcher, T., (2012). High Sr/Y magmas reflect arc maturity, high magmatic water content, and porphyry  $\text{Cu} \pm \text{Mo} \pm \text{Au}$  potential: examples from the Tethyan arcs of central and eastern Iran and western Pakistan. *Economic Geology*, 107, 295-332.
- [12] Asiabanha, A., Foden, J., (2012). Post-collisional transition from an extensional volcanosedimentary basin to a continental arc in the Alborz Ranges, N-Iran. *Lithos* 148, 98-111.
- [13] Ghafaribijar, S., (2009). *Geochemistry of Potassic Mafic Rocks in the Lar Complex, North of Zahedan, East of Iran*. M.Sc. Thesis, Sistan and Baluchestan Univ.
- [14] Pang, K. N., Chung, S. L., Zarrinkoub, M. H., Khatib, M. M., Mohammadi, S. S., Chiu, H. Y., Chu, C. H., Lee, H. Y. and Lo, C. H., (2013). Eocene-Oligocene post-collisional magmatism in the Lut-Sistan region, eastern Iran: Magma genesis and tectonic implications. *Lithos*, 180-181, 234-251.
- [15] Stone, D., (2000). Temperature and pressure variations in suites of Archean felsic plutonic rocks, Berens river area, northwest superior province, Ontario, Canada. *The Canadian Mineralogist*, 38, 455-470.
- [16] Deer, W. A., Howie, A., Zussman, J., (1986). *An introduction to rock-forming minerals*. 17th edn. Longman Ltd, 528p.
- [17] Abdel-Rahman, A. M., (1994). Nature of biotites from alkaline, calc-alkaline, and peraluminous magmas, *Journal of Petrology*, 35, 2, 525-541.
- [18] Foley, S. F., Venturelli, G., Green, D. H., Toscani, L., (1987). The ultrapotassic rocks: characteristics, classification, and constraints for petrogenetic models. *Earth-Sciences Reviews*, 24, 81-134.
- [19] Engel, A. E. J., Engel, C. G., (1960). *Progressive metamorphism and granitization of the major paragneiss, northwest Adirondack Mountains, New York, Part 2. Mineralogy*. *Bulletin of the Geological Society of America*, 71, 1.58.
- [20] Kwak, T. A. P., (1968). Ti in biotite and muscovite as an indication of metamorphic grade in almandine amphibolite facies rocks from Sudbury, Ontario. *Geochimica et Cosmochimica Acta*, 32, 1222-1229.
- [21] Robert, J. L., (1976). Titanium solubility in synthetic phlogopite solid solutions. *Chemical Geology*, 17, 213-227.
- [22] Dymek, R. F., (1983). Titanium, aluminum and interlayer cation substitutions in biotite from high-grade gneisses, West Greenland. *American Mineralogist*, 68, 880-899.
- [23] Guidotti, C. V., Sassi, F. P., (2002). Constraints on studies of metamorphic K-Na white micas. In A. Mottana, F.P. Sassi, J.B. Thompson Jr., and S. Guggenheim, Eds., *Micas: Crystal Chemistry and Metamorphic Petrology*, 46, 419-448. *Reviews in Mineralogy and Geochemistry*, Mineralogical Society of America, Washington, D. C.
- [24] Henry, D. J., and Guidotti, C. V., (2002). Ti in biotite from metapelitic rocks: Temperature effects, crystallochemical controls and petrologic applications. *American Mineralogist*, 87, 375-382.
- [25] Uchida, E., Endo, S., Makino, M., (2007). Relationship between solidification depth of granitic rocks and formation of hydrothermal ore deposits. *Resource Geology*, 57, 1, 47-56.
- [26] Arima, M., Edgar, A. D., (1981). Substitution mechanisms and solubility of titanium in phlogopites from rocks of probable mantle origin. *Contributions to Mineralogy and Petrology*, 77, 288-295.
- [27] Tronnes, R. G., Edgar, A. D., Arima, M., (1985). A high pressure-high temperature study of  $\text{TiO}_2$  solubility in Mg-rich phlogopite: Implications to phlogopite chemistry. *Geochimica et Cosmochimica Acta*, 49, 2323-2329.